Architectural integration of photovoltaics: performance evaluation of curved modules.

Marco Lovati – Institute for Renewable Energy, eurac research – marco.lovati@eurac.edu
Laura Maturi – Institute for Renewable Energy, eurac research – laura.maturi@eurac.edu
David Moser – Institute for Renewable Energy, eurac research – david.moser@eurac.edu

Abstract

BiPV (Building integrated photovoltaics) stands on the bridge between architecture and energy production, some photovoltaic companies in the last decade are engaging in the design and production of non conventional PV technologies (Cerón, Caamaño-Martín, and Neila 2013). BiPV industry aims to transform PV from power plant to building material, thus is coming up the need for features such as freedom of color and dimensions, and flexibility. In this paper a method is presented for the estimation of power production on curved active surfaces, the performance of two samples of flexible thin film photovoltaic modules are evaluated as a validation. Because of its curved application, the performance of the modules under study is affected by electrical layout and non-uniform temperature issue. The work shows a method to simulate the performance of curved photovoltaic modules subject to uneven irradiation. For the experimental set-up, a curved shelter was built (of those typically used to shield market carts outside of supermarkets). Two different flexible photovoltaic modules are glued onto the curved roof of the structure, each module is equipped with an MPPT tracker connected to a data logger, there are then 2 thermocouples to measure temperatures in the two different modules. Because of the curved shape of the photovoltaic surface the incoming irradiation cannot be measured with a pyranometer, and should therefore be accessed by geometry based computer simulation. The irradiation is simulated using ray-tracing computations (Ward 1996). The simulation uses weather data retrieved from the weather station located at the ABD airport in Bozen (less then 1 Km away). The main result is the comparison between the simulated power production and the measured one. Both simulated and measured power, points to a better performance linked to one electrical layout over the other. More values are of interest such as Ross coefficient on the module for this particular type of shape and integration. The study shows an acceptable level of agreement between the simulated power production and the measured one provided that some parameters are calibrated. The possibility of simulating this technology opens the path for economic analysis and feasibility studies to access the real potential of this technology in non-flat application cases.

1. Introduction

Performance prediction and monitoring of PV performance at a system level is crucial for effective management of renewable energy in both design and operation phase. Well established guidelines, standards and good practices are available for the assessment of performances and the calibration of parameters in a model (Woyte et al. 2013). Research literature present numerous studies about the accuracy of instruments and uncertainty of measurement. Nevertheless, can happen that the shape of the PV system is complex and some key aspects are not known by simple measurements. This is the case for flexible PV modules glued on a curved surface Fig. 1, the incoming irradiance cannot be measured along the whole surface but needs to be estimated by means of computer simulation. The present study aims at showing a versatile and lean modelling and simulation procedure for the assessment of performances in non-conventional PV modules and systems. The method is particularly desirable for optimization purposes where the computational time is critical.

2. Methodology

2.1 Experimental setup

In the field test the modules are bent over a curved surface (i.e. the ceiling of a shopping cart's shelter of those typically found outside supermarkets) as in Fig. 1.

Fig. 1 – photo of the experimental setup

The curvature of the modules is aligned north-south so that each part of the module gets irradiated mainly in a particular time of the day, at noon the irradiation pattern is symmetrical over the module and the most irradiated spot is the centre. Each of the two modules is connected to an MPPT device equipped with a data logger that collects the power production each minute, the loggers are then connected to a battery which in turn is connected to a dissipating load. The two modules share the same CIGS cell technology but are differently organized at the module level as shown in Fig. 2. M1 is transversally divided in 14 smaller modules connected in parallel with each other, while M2 is transversally divided in 44 cells connected in series. The arrangement of M2 may cause huge losses and overheating problems (hot spots) in strongly asymmetrical irradiation conditions, to mitigate these problems the manufacturer equipped each pair of cells with a bypass diode for a total number of 22 diodes.

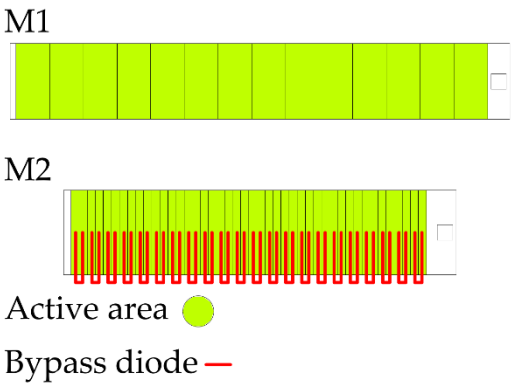

Fig. 2 – module level organization of the two technologies.

Each module is equipped with a thermocouple to measure the superficial temperature on its horizontal edge. Parameters such as ambient temperature, GH and DN are retrieved from the ABD meteorological station located about one km south of the test field.

2.2 Model and formulas

The performance modelling and assessment methods, are based on the estimate of the incoming irradiation on the plane of the module (Sprenger, Wilson, and Kuhn 2016). Usually trigonometric formulas are used to estimate the irradiation, these could become particularly cumbersome in case of a curved surface. The computation could be sped by simply dividing the curved surface into a number of flat patches. In this paper though a backward ray-tracing procedure using the software Radiance (Ward 1996) was adopted, the main advantage of this approach is that it is geometry independent (i.e. can be performed independently from the geometry on which the radiation is calculated and on the shading bodies), is therefore particularly fit for BIPV applications. The two modules were modelled by approximating the curved surface with a series of flat portions as in Fig. 3, to each portion corresponds one measuring point. The ray tracing procedure is used in this case to retrieve daylight coefficients between each measuring point and different part of the sky vault using the software Daysim (Reinhart and Herkel 2000), this method allows for computing the irradiation over different timesteps with one only ray tracing calculation.
Once the irradiation on the different portions of the modules in every timestep of the analysis period is known the power production of the two modules can be estimated.

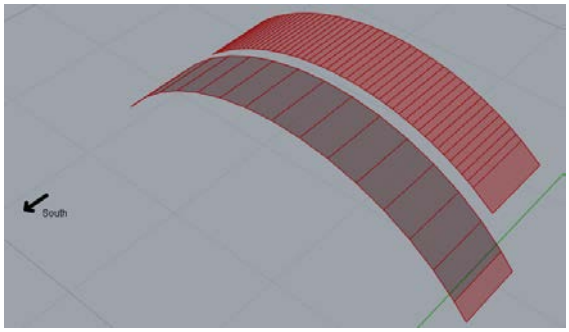

Fig. 3 – model construction of the two modules and approximation of the curved surface with a discrete number of flat portions

2.2.1 M1

As said the first module is formed by 14 smaller modules connected in parallel to each other, this disposition renders the power production strongly correlated to the average irradiation over the surface. To model the behavior of this technology a simple relation such as the following is shown to yield satisfying results, the power of the M1 module over one timestep "t" is therefore:

$$P(t) = A \cdot \eta \cdot N^{-1} \cdot \sum_{i=1}^{N} I_i \cdot c(T) \quad (1)$$

Where c(T) was calibrated to better match the experimental data and found equal to - 0.002 °K.

2.2.2 M2

The second module presents a power production that is not proportional to the average irradiation as it is influenced by the electrical disposition of its cells, to model the behavior of M2 was used, as an approximation, the following relation:

$$P(t) = \min(I_i \cdot c(T)) \cdot A \cdot \eta \quad (2)$$

In this case c(T) was assumed equal to the one from M1.

In this model the least electrically producing cell in the module dominates the production output of the system, the model does not take into account the behavior of the bypass diode provoking an underestimation of the power during the morning and the evening. In this equation the temperature effect is not taken into account as the estimation of the temperature gradient along the module is strongly dependent on the formation of hot-spot and on the behavior of the bypass diode.

2.2.3 module temperature assessment

Given the present scarcity of thermal sensors in operational commercial PV systems, the estimation of the temperatures of the modules in the simulation make sense from a technical standpoint. Furthermore the sensors were positioned only in the center of the module, thus ignoring a temperature gradient along the module length, this gradient could be accesed by estimating temperatures. Some correlations exist to access the superficial temperature of one module (Skoplaki and Palyvos 2009), among these the most straightforward was used:

$$T_{MOD} = T_{AMB} + k \cdot G \quad (3)$$

The Ross coefficient (Ross and Smokler 1986)was retrieved by linear interpolation of the difference in temperature (T_{AMB}-T_{MOD}) against the corresponding irradiation. Where a thermal sensor is not available the following empirical equation can be used:

$$k = (NOCT - 20)/800 \quad (4)$$

3. results

The power production from the two modules are shown and compared with the results of the simulation method applied.

3.1 Ross Coefficient

As with other semiconductor devices, higher temperatures reduce the power output of PV. The power reduction in the case of PV happens in an almost linear way (Skoplaki, Boudouvis, and Palyvos 2008).

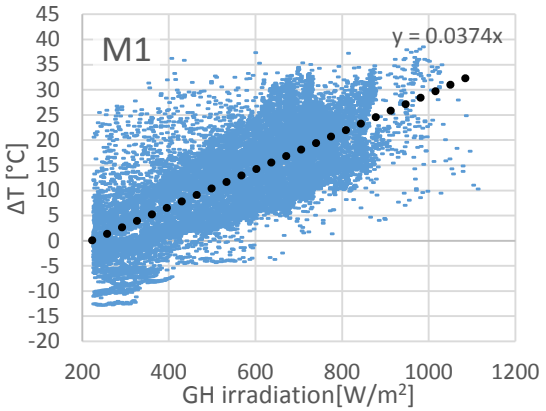

Fig. 4– $\Delta T=(T_{MOD}-T_{AMB})$ versus irradiation for M1

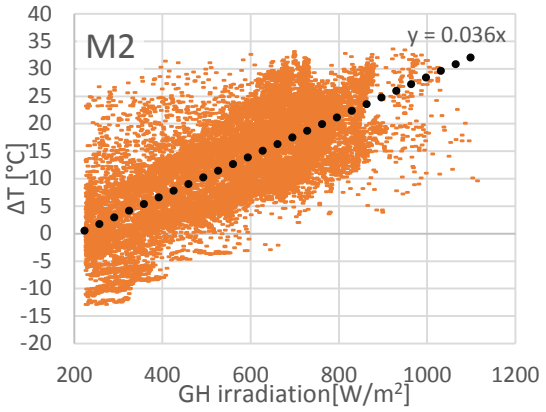

Fig. 5– $\Delta T= (T_{MOD}-T_{AMB})$ versus irradiation for M2

Because both the technologies indicate a NOCT of 48°C , the Ross coefficient k would result equal to 0.035°C/(W/m²). The results show in accordance with values for a flat plate rack mounted CIGS module (Maturi et al. 2014), indicating that there is no detectable overheating caused by the type of integration.

3.2 Field Test results

3.2.1 Measured electricity production

From the data collected by the loggers is possible to have an idea about the performances of the two modules. Examining the production curves in a clear sky day a difference is apparent Fig. 4. The difference exist despite a similar shape and irradiation pattern because of the electrical layout.

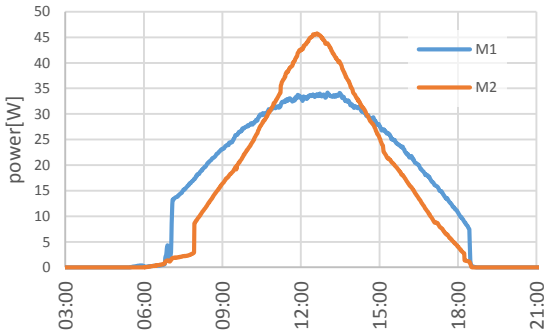

Fig. 6 – it is shown the power output of the two modules for August 8th 2016.

In general M2 technology outperforms the other around noon generating a narrower and somewhat sharper profile. Given the higher nominal power declared by the producer (M1=47 W, M2=70 W), which is almost proportional to the highest power at noon (e.g. M1 = 33 W, M2 = 45 W), it is plausible that M2 suffers a drop in efficiency during morning and afternoon. This could be explained by stronger current mismatch effects when the irradiation pattern is more asymmetrical (i.e. the sun is east or west). Considering the cumulative energy production over an analysis period of 10 days (from August 26th to September 5th 2016) M1 shown a higher energy production (M1≈ 126 kWh M2≈ 117 kWh).

3.2.2 Simulated electricity production

The simple formula used in equation 1 show a good level of agreement with the measured data. An overestimation of the power is apparent during the morning hours, this is due to a lag in the sunrise time between the location of the experiment and the pyrheliometer at ABD.

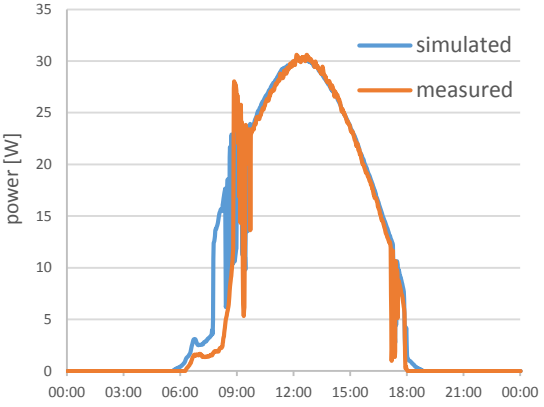

Fig. 7–simulated and measured power output for the M1 module for August the 31st.

The error in the days from August 26th to September 5th 2016 was analyzed. Filtering the data and keeping only the core hours (from 9:30 to 15:30) the simulated power production and the measured one show are shown in Fig. 8.

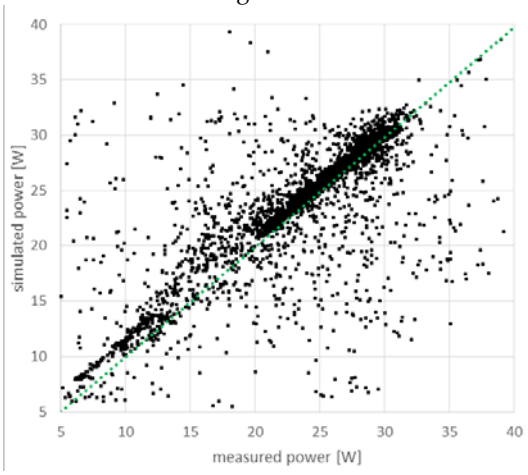

Fig. 8 dispersion diagram of simulated vs measured power from August 26th to September 5th 2016. The data had been filtered removing the morning hours.

The error (measured – simulated power) resulted from a Kolmogorov-Smirnov test of significance level 0.1 to be drawn from a normal population of mean -0.28 W and standard deviation 1 W.

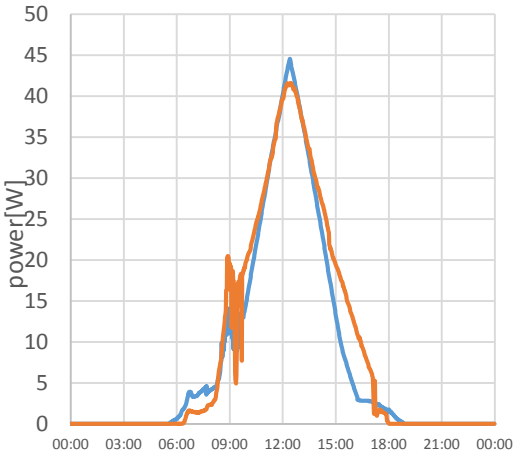

Fig. 9– simulated and measured power output for the M2 module for August the 31st.

The simulation of the M2 technology has proven less successful for a straightforward approach like the one proposed. Equation 2 in fact assumes that the power produced by every cell is equal to the least irradiated one, this does not coincide with the real behavior because of the presence of bypass diodes. The simplification in modeling leads to a severe underestimation of the output power in the hours far from noon.

4. Conclusions

The integration of this flexible technology in direct contact with a curved polycarbonate board do not show significant overheating problems compared with a standard free field application, therefore the need for ventilation is not an issue for this specific use.

The on-field data collected shows an higher cumulative energy production from the technology M1 despite a lower nominal power, the efficiency loss is shown to be due to the electric layout of M2.

The integration of the ray-tracing techniques in the photovoltaic simulation at module scale proves successful for the technology M1 while M2 needs a deeper electrical modelling of the bypass diodes to avoid an underestimation of the electricity production. Is unclear whether a fast and straightforward approach can lead to sufficiently accurate results, it depends on the computational cost of simulating a substantial number of bypass diodes. A lean approach is needed because is computationally fit for optimization processes.

5. Acknowledgement

This study was developed within commonenergyproject and has received funding from the European Union Seventh Framework Programme FP7/2007-2013 under Grant Agreement 608678.

6. Nomenclature

A	area of the module
ABD	areoporto Bolzano Dolomiti
c(T)	temperature correction coeffiient
CIGS	copper indium gallium selenide
DN	direct normal irradiation
G	global radiation
GH	Global-horizontal irradiation
I	irradiation
k	ross coefficient
M1	module of the 1st technology
M2	module of the 2nd technology
MPP	maximum power point
MPPT	maximum power point tracker
N	number of cells in the module
NOCT	normal operating cell temperature
OC	open circuit
SC	short circuit
T_{AMB}	ambient temperature
T_{MOD}	temperature of module
η	efficiency of the cell

7. References

Cerón, Isabel, E. Caamaño-Martín, and F. Javier Neila. 2013. "'State-of-the-Art' of Building Integrated Photovoltaic Products." *Renewable Energy* 58 (October): 127–33. doi:10.1016/j.renene.2013.02.013.

Maturi, Laura, Giorgio Belluardo, David Moser, and Matteo Del Buono. 2014. "BiPV System Performance and Efficiency Drops: Overview on PV Module Temperature Conditions of Different Module Types." *Energy Procedia*, Proceedings of the 2nd International Conference on Solar Heating and Cooling for Buildings and Industry (SHC 2013), 48: 1311–19. doi:10.1016/j.egypro.2014.02.148.

Reinhart, Christoph F., and Sebastian Herkel. 2000. "The Simulation of Annual Daylight Illuminance Distributions — a State-of-the-Art Comparison of Six RADIANCE-Based Methods." *Energy and Buildings* 32 (2): 167–87. doi:10.1016/S0378-7788(00)00042-6.

Ross, R. G., and M. I. Smokler. 1986. "Electricity from Photovoltaic Solar Cells: Flat-Plate Solar Array Project Final Report. Volume VI: Engineering Sciences and Reliability." Report or Paper. October. http://resolver.caltech.edu/CaltechAUTHORS:JPLpub86-31-volumeVI.

Skoplaki, E., A.G. Boudouvis, and J.A. Palyvos. 2008. "A Simple Correlation for the Operating Temperature of Photovoltaic Modules of Arbitrary Mounting." *Solar Energy Materials and Solar Cells* 92 (11): 1393–1402. doi:10.1016/j.solmat.2008.05.016.

Skoplaki, E., and J.A. Palyvos. 2009. "Operating Temperature of Photovoltaic Modules: A Survey of Pertinent Correlations." *Renewable Energy* 34 (1): 23–29. doi:10.1016/j.renene.2008.04.009.

Sprenger, Wendelin, Helen Rose Wilson, and Tilmann E. Kuhn. 2016. "Electricity Yield Simulation for the Building-Integrated Photovoltaic System Installed in the Main Building Roof of the Fraunhofer Institute for Solar Energy Systems ISE." *Solar Energy* 135 (October): 633–43. doi:10.1016/j.solener.2016.06.037.

Ward, G. 1996. "RADIANCE Reference Manual." *IEA SHC Task* 12.

Woyte, Achim, Mauricio Richter, David Moser, Stefan Mau, Nils Reich, and Ulrike Jahn. 2013. "Monitoring of Photovoltaic Systems: Good Practices and Systematic Analysis." In *Proc. 28th European Photovoltaic Solar Energy Conference*, 3686–3694.